Modal-reflectivity enhancement by geometry tuning in Photonic Crystal microcavities

Christophe Sauvan, Guillaume Lecamp, Philippe Lalanne, Jean-Paul Hugonin

Modal-reflectivity enhancement by geometry tuning in Photonic Crystal microcavities

C. Sauvan, G. Lecamp, P. Lalanne and J.P. Hugonin

Laboratoire Charles Fabry de l'Institut d'Optique, Université Paris Sud bât. 503
Centre National de la Recherche Scientifique, F-91403 Orsay Cedex, France
philippe.lalanne@iota.u-psud.fr

Abstract: When a guided wave is impinging onto a Photonic Crystal (PC) mirror, a fraction of the light is not reflected back and is radiated into the claddings. We present a theoretical and numerical study of this radiation problem for several three-dimensional mirror geometries which are important for light confinement in micropillars, air-bridge microcavities and two-dimensional PC microcavities. The cause of the radiation is shown to be a mode-profile mismatch. Additionally, design tools for reducing this mismatch by tuning the mirror geometry are derived. These tools are validated by numerical results performed with a three-dimensional Fourier modal method. Several engineered mirror geometries which lower the radiation loss by several orders of magnitude are designed.

OCIS codes: (130.3120) Integrated optics devices; (230.3990) Microstructure devices; (230.5750) Resonators; (140.4780) Optical resonators

References and links

1. K.J. Vahala, "Optical microcavities," Nature **424**, 839-846 (2003).
2. J.P. Zhang, D.Y. Chu, S.L. Wu, W.G. Bi, R.C. Tiberio, R.M. Joseph, A. Taflove, C.W. Tu, S.T. Ho, "Nanofabrication of 1-D photonic bandgap structures along a photonic wire," IEEE Photon. Technol. Lett. **8**, 491-493 (1996).
3. J.S. Foresi, P.R. Villeneuve, J. Ferrera, E.R. Thoen, G. Steinmeyer, S. Fan, J.D. Joannopoulos, L.C. Kimerling, H.I. Smith and E.P. Ippen, "Photonic-bandgap microcavities in optical waveguides," Nature **390**, 143-145 (1997).
4. T.F. Krauss, O. Painter, A. Scherer, J.S. Roberts, R.M. De La Rue, "Photonic microstructures as laser mirrors," Opt. Eng. **37**, 1143-1148 (1998).
5. T. Baba, M. Hamasaki, N. Watanabe, P. Kaewplung, A. Matsutani, T. Mukaihara, F. Koyama and K. Iga, "A novel short-cavity laser with deep-grating distributed Bragg reflectors," Jpn. J. Appl. Phys. **35**, 1390-1394 (1996).
6. B.E. Little, H.A. Haus, J.S. Foresi, L.C. Kimerling, E.P. Ippen and D.J. Ripin, "Wavelength switching and routing using absorption and resonance," IEEE Phot. Technol. Lett. **10,** 816-818 (1998).
7. Y. Akahane, T. Asano, B.S. Song and S. Noda, "Investigation of high-Q channel drop filters using donor-type defects in two-dimensional photonic crystal slabs," Appl. Phys. Lett. **83**, 1512-1514 (2003).
8. H.G. Park, J.K. Hwang, J. Huh, H.Y. Ryu, Y.H. Lee and J.S. Kim, "Nondegenerate monopole-mode two-dimensional photonic band gap laser," Appl. Phys. Lett. **79**, 3032-3034 (2001).
9. J.M. Gérard, and B. Gayral, "Strong Purcell Effect for InAs quantum boxes in three-dimensional solid-state microcavities," J. Lightwave Technol. **17**, 2089-2095 (1999).
10. G.S. Solomon, M. Pelton and Y. Yamamoto, "Single-mode spontaneous emission from a single quantum dot in a three-dimensional microcavity," Phys. Rev. Lett. **86**, 3903-3906 (2001).
11. S.G. Johnson, S. Fan, A. Mekis and J. D. Joannopoulos, "Multipole-cancellation mechanism for high- Q cavities in the absence of a complete photonic band gap," Appl. Phys. Lett. **78**, 3388-3300 (2001).
12. K. Srinivasan, O. Painter, "Momentum space design of high-Q photonic crystal optical cavities," Opt. Exp. **10**, 670-684 (2002), http://www.opticsexpress.org/abstract.cfm?URI=OPEX-10-15-670
13. J. Vuckovic, M. Loncar, H. Mabuchi and A. Scherer, "Optimization of the Q factor in Photonic Crystal microcavities," IEEE J. Quantum Electron. **38**, 850-856 (2002).
14. Y. Akahane, T. Asano, B.S. Song and S. Noda, "High-Q photonic nanocavity in two-dimensional photonic crystal," Nature **425**, 944-947 (2003).

#5572 - $15.00 US Received 25 October 2004; revised 22 December 2004; accepted 30 December 2004

15. P. Lalanne, S. Mias and J.P. Hugonin, "Two physical mechanisms for boosting the quality factor to cavity volume ratio of photonic crystal microcavities," Opt Express **12**, 458-467 (2004), http://www.opticsexpress.org/abstract.cfm?URI=OPEX-12-3-458
16. M. Palamaru and P. Lalanne, "Photonic crystal waveguides: out-of-plane losses and adiabatic modal conversion," Appl. Phys. Lett. **78**, 1466-1469 (2001).
17. P. Lalanne and J. P. Hugonin, "Bloch-wave engineering for high Q's, small V's microcavities," IEEE J. Quantum Electron. **39**, 1430-1438 (2003).
18. E. Silberstein, P. Lalanne, J.P. Hugonin and Q. Cao, "On the use of grating theory in integrated optics," J. Opt. Soc. Am. A. **18**, 2865-28275 (2001).
19. Q. Cao, P. Lalanne and J.P. Hugonin, "Stable and efficient Bloch-mode computational method for one-dimensional grating waveguide," J. Opt. Soc. Am. A **19**, 335-338 (2002).
20. W.C. Chew and W.H. Weedon, "A 3D perfectly matched medium from modified Maxwell's equations with stretched coordinates," Microwave Opt. Technol. Lett. **7**, 599-604 (1994).
21. N. Château and J.P. Hugonin, "Algorithm for the rigorous coupled-wave analysis of grating diffraction," J. Opt. Soc. Am. A **11**, 1321-1331 (1994).
22. L. Li, "Use or Fourier series in the analysis of discontinuous periodic structures," J. Opt. Soc. Am. A **13**, 1870-1876 (1996).
23. P. Lalanne and G.M. Morris, "Highly improved convergence of the coupled-wave method for TM polarization," J. Opt. Soc. Am. A **13**, 779-784 (1996).
24. L. Li, "New formulation of the Fourier modal method for crossed surface-relief gratings," J.Opt. Soc. Am. A **14**, 2758-2767 (1997).
25. P. Lalanne, "Effective properties and band structures of lamellar subwavelength crystals: plane-wave method revisited," Phys. Rev B **58**, 9801-9807 (1998).
26. E. Popov and M. Nevière, "Grating theory: new equations in Fourier space leading to fast converging results for TM polarization," J. Opt. Soc. Am. A **17**, 1773-1784 (2000).
27. J. Ctyroky, S. Helfert, R. Pregla, P. Bienstman, R. Baets, R. De Ridder, R. Stoffer, G. Klaasse, J. Petracek, P. Lalanne, J.P. Hugonin, R.M. De La Rue, "Bragg waveguide grating as a 1D photonic band gap structure: COST 268 modelling task," Opt. Quant. Electron. **34**, 455-470 (2002).
28. C. Sauvan, P. Lalanne, J.C. Rodier, J.P. Hugonin and A. Talneau, "Accurate modeling of line-defect Photonic Crystal waveguides," IEEE Photon. Technol. Lett. **15**, 1243-1245 (2003).
29. P. Lalanne, "Electromagnetic analysis of photonic crystal waveguides operating above the light cone," IEEE J. Quantum Electron. **38**, 800-804 (2002).
30. A. Yariv and P. Yeh, *Optical waves in crystals* (John Wiley & Sons, New York, 1984).
31. A. Chutinan and S. Noda, "Waveguides and waveguide bends in two-dimensional photonic crystal slabs," Phys. Rev. B **62**, 4488-4492 (2000).
32. M. Notomi, K. Yammada, A. Shinya, J. Takahashi, C. Takayashi and I. Yokohama, "Extremely large group-velocity dispersion of line-defect waveguides in photonic crystal slabs," Phys. Rev. Lett. **87**, art. #253902 (2001).
33. C. Sauvan, P. Lalanne and J.P. Hugonin, "Tuning holes in Photonic Crystal nanocavities," Nature **429**, 1 (2004).
34. H.Y. Ryu, M. Notomi, E. Kuramoti and T. Segawa, "Large spontaneous emission factor (>0.1) in the photonic crystal monopole-mode laser," Appl. Phys. Lett. **84**, 1067-1069 (2004).
35. P. Lalanne, J.P. Hugonin and J.M. Gérard, "Electromagnetic study of the Q of pillar microcavities in the small limit diameter," Appl. Phys. Lett. **84**, 4726-4728 (2004).
36. J. Vuckovic, M. Pelton, A. Scherer, and Y. Yamamoto, "Optimization of three-dimensional micropost microcavities for cavity quantum electrodynamics," Phys. Rev. A **66**, #023808 (2002).
37. E. Aarts and J. Korst, *Simulated Annealing and Boltzmann Machine* (John Wiley & Sons, New York 1989).

1. Introduction

One of the greatest challenges in Photonic Crystal (PC) research is the construction of optical microcavities with small modal volumes and large quality factors for an efficient confinement of light and for efficient light-matter interaction. Besides standard applications of these structures as lasers or frequency filters, they can potentially be used in solid-state quantum electrodynamics or in nonlinear light-control experiments [1]. For cavity geometries like microtoroids or microdisks, the confinement is purely refractive. These geometries will not be discussed hereafter. Over the past decade, many research groups have focused their efforts on PC cavities which can be fabricated with standard planar technologies [2-10]. In all these systems, see Fig. 1, the light confinement has a hybrid character: it relies on refraction (total internal reflection) and diffraction. For air-bridge [2-3] or micropillar cavities [9-10] shown in Figs. 1a and 1b, light is confined by refraction in two orthogonal directions and by two 1D PC mirrors in the third direction. For the membrane structure [7-8] shown in Fig. 1c, light is

#5572 - $15.00 US Received 25 October 2004; revised 22 December 2004; accepted 30 December 2004

confined in two in-plane directions by diffraction and in the vertical direction by refraction. The main consequence of this hybrid confinement is the presence of far-field radiation in the air-clads, which limits the cavity mode lifetime.

Previous theoretical works devoted to the analysis of the radiation problem for enhancing the cavity mode lifetime emphasize a global property of the cavity mode. They all begin with a preliminary calculation of the mode pattern followed by an interpretation of this pattern through a multipole expansion [11] or a Fourier decomposition [12-14]. The approach we adopt here is largely different since we emphasize an intrinsic property of the mirrors, namely their modal reflectivity. Looking at mirrors properties is all the more natural since the use of mirrors with a high modal reflectivity guarantees a high performance cavity. For the geometries of Figs. 1a and 1b, the modal reflectivity we consider is that of a guided mode impinging onto a 1D Bragg mirror, see Figs. 5b and 6a, and for the geometry of Fig. 1c we consider the modal reflectivity of a guided Bloch mode impinging onto a 2D PC mirror, see Fig. 5(a). Our purpose is not to understand the cavity mode in these ultrasmall cavities as simply resulting from the bouncing of a guided wave between two mirrors ; counterexamples of such simplistic approaches are known [15]. We rather intend to explain the physical origin for the imperfect (< 1) modal reflectivity and to derive engineering tools to increase it or equivalently to reduce the radiation losses down to a very low level (< 0.1% of the incident energy). Similar concepts have been developed earlier for 2D geometries composed of 1D Bragg mirrors in planar waveguides [16-17], and this work represents an extension to several 3D geometries which are conceptually more difficult to handle and also more relevant for applications. The origin of the finite mirror reflectivity, namely a transverse mode-profile mismatch at the mirror termination, is theoretically analysed in Section 2 for the air-bridge geometry. From this analysis, we propose in Section 3 design rules for reducing the mode-profile mismatch. In Section 4, these rules are validated with three-dimensional computational results obtained for several mirror geometries, including 1D Bragg mirrors in cylindrical and rectangular photonic wires and 2D PC mirrors in membranes.

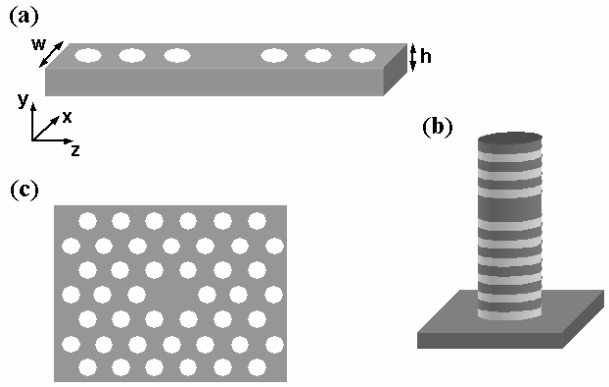

Fig. 1. Optical microcavities considered in this work. (a) Air-bridge microcavity. (b) Micropillar. (c) Single defect PC microcavity in a semiconductor membrane (top view).

In the following, the calculations of the modal reflectivities are performed with a 3D frequency-domain modal method relying on Fourier expansion techniques [18-19]. In brief, the Fourier-expansion method relies on an analytical integration of Maxwell's equations along one direction (usually the longitudinal direction of the waveguide) and on a supercell approach in the other two transversal directions. Perfectly-Matched-Layers [20] are used in those directions to carefully handle the far-field radiation losses and to satisfy outgoing wave conditions at the supercell boundaries. Since these layers absorb non-evanescent radiations, the electromagnetic fields are null on the boundaries of the supercell and are thus periodic functions of the transversal coordinates. This allows the calculation of the radiated and guided modes in a Fourier (plane-wave) basis in each layer and the integration in the longitudinal

#5572 - $15.00 US Received 25 October 2004; revised 22 December 2004; accepted 30 December 2004

direction by relating recursively the modes amplitudes in the different layers using a S-matrix approach [21]. We use the mathematically-sound Fourier factorization rules [22] which are known to drastically improve the convergence performance of Fourier-expansion techniques for Bloch waves computation in periodic media [23-26]. This 3D frequency-domain modal method has been checked for different geometries through comparison with other numerical methods [27-28] and with experimental data [18].

2. Mode-profile mismatch problem

In this Section, we consider the air-bridge geometry of Fig. 1(a) and evidence the physical reason for the radiation losses occurring when light guided in the bridge reflects onto the semi-infinite mirror. The computational results are obtained for a 340-nm-thick, 500-nm-wide air-bridge, and the periodicity constant and the hole diameter of the mirror are a = 420 nm and d = 230 nm, respectively. The semiconductor refractive index (n = 3.48) is assumed to be independent of the wavelength, an approximation largely inessential for the following discussion. In the wavelength range of interest, the waveguide supports a single TE-like mode (electric field primarily horizontal at the center of the waveguide) with a double mirror symmetry. Figure 2(a) shows the calculated modal reflectivity R of the PC mirror as a function of the wavelength over the entire band gap from λ = 1.39 to 1.84 μm. The modal reflectivity does not reach unity, and L = 1-R simply represents radiation losses in the air-clad.

Before considering reflectivity enhancement through hole tuning, let us evidence that the cause of the non-perfect reflectivity of the semi-infinite mirror is a mode-profile mismatch at the waveguide-mirror interface between the air-bridge guided mode and the Bloch mode of the mirror (sometimes called impedance mismatch). For that purpose, we use an analytical model developed earlier for simpler 2D geometries [16]. Within the model, light reflection on a PC mirror is interpreted as a triple scattering process and the radiation losses L are shown to be equal to $1-\eta^2$, where

$$\eta = \frac{\Re e\left\{\left[\iint dxdy\left(\mathbf{E}_1\times\mathbf{H}_T^{\,*}\right)\mathbf{e}_z \iint dxdy\left(\mathbf{E}_T\times\mathbf{H}_1^{\,*}\right)\mathbf{e}_z\right] \Big/ \left[\iint dxdy\left(\mathbf{E}_T\times\mathbf{H}_T^{\,*}\right)\mathbf{e}_z\right]\right\}}{\Re e\left\{\iint dxdy\left(\mathbf{E}_1\times\mathbf{H}_1^{\,*}\right)\mathbf{e}_z\right\}} \qquad (1)$$

is an overlap integral between the incident guided mode and the half-Bloch wave of the mirror, an electromagnetic quantity associated to the fundamental evanescent Bloch mode of the mirror, see Ref. [16] for a definition of half-Bloch waves. In Eq. (1), $\mathbf{e_z}$ is the longitudinal unitary vector, $\mathbf{E_1}$ and $\mathbf{H_1}$ respectively represent the transverse electric and magnetic fields of the fundamental air-bridge mode and $\mathbf{E_T}$ and $\mathbf{H_T}$ represent those of the half-Bloch wave. We have calculated these transverse fields with the Fourier modal method. Details concerning the calculation of the Bloch mode can be found in Refs. [19, 29]. From those fields, we have computed the square of the overlap integral. The y-component of $\mathbf{H_1}$ and $\mathbf{H_T}$ is shown in Figs. 2(b)-2(f) for several wavelengths over the whole bandgap of the PC mirror and the η^2 values are represented by blue circles in Fig. 2(a). Clearly, a quantitative agreement with the exact numerical data (solid curve) is achieved. From Fig. 2(a), we note that the radiation losses increase as the wavelength decreases in the gap. This effect can be simply understood from classical results known for Bloch modes in thin-film stacks [30]: as the wavelength decreases in the gap, the fundamental Bloch mode of the air-bridge mirror becomes less and less confined in the high index material, and spreads out into the air clad and the holes. Thus the mode-profile mismatch between the Bloch mode and the air-bridge guided mode becomes more and more severe, as evidenced in Figs. 2(b)-2(f).

#5572 - $15.00 US Received 25 October 2004; revised 22 December 2004; accepted 30 December 2004

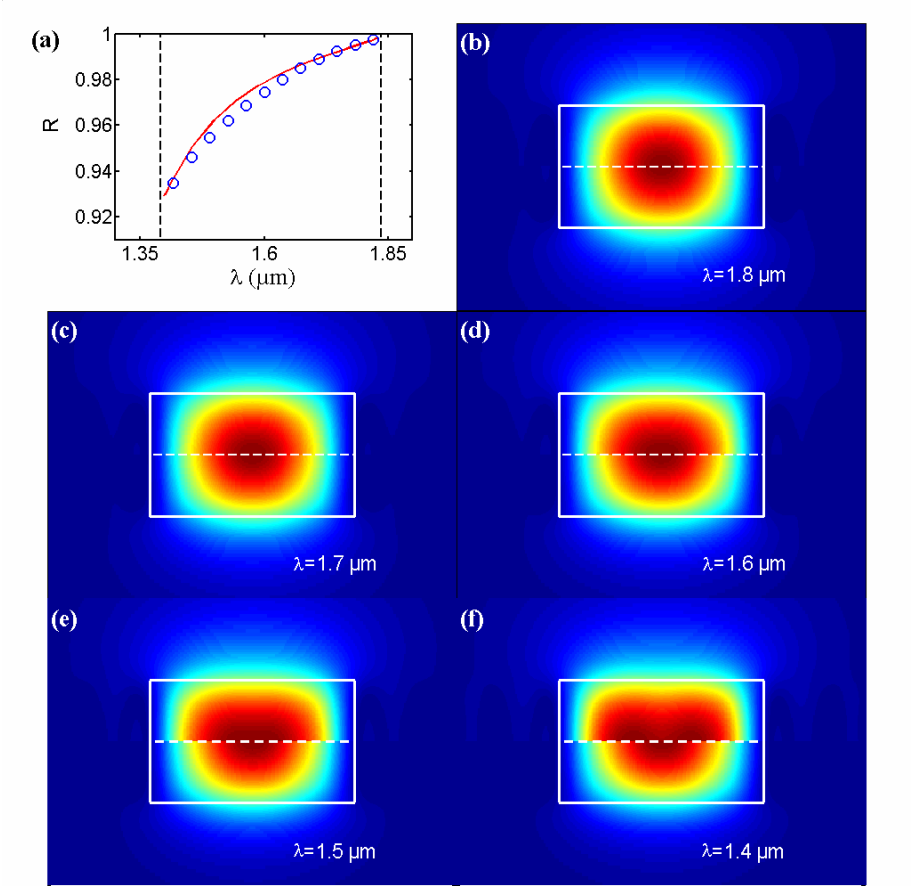

Fig. 2. Modal reflectivity and transverse mode-profile mismatch. (a) Modal reflectivity spectrum for the air-bridge mirror (a = 420 nm and d = 230 nm). Solid red curve: computational data using exact electromagnetic theory. Blue circles: square of the overlap integral η^2. The vertical dashed lines indicate the band edges. (b)-(f) Comparison between the y-component of the transverse magnetic field of the fundamental air-bridge mode $\mathbf{H}_1$ (bottom) and that of the half-Bloch wave $\mathbf{H}_T$ (top) for several wavelengths covering the whole bandgap. White solid lines indicate the semiconductor-air boundaries of the air-bridge. The transverse $\mathbf{H}_T$ field is calculated in a symmetry plane shown as vertical dashed lines in the left-hand side of Fig. 3.

3. Bloch mode engineering for lowering radiation losses

The mode-profile mismatch problem shows the necessity of designing mirrors which incorporate modal conversion to reduce the radiation losses. This modal conversion can be implemented by a gradual variation of the mirror geometry aimed at tapering the incident guided mode into the fundamental evanescent Bloch mode of the mirror [16-17]. A mirror incorporating such a progressive variation between the air-bridge waveguide and the semi-infinite periodic Bragg mirror is shown in Fig. 3. To analyse this geometry, a convenient approach consists in identifying segments (delimited by vertical dashed lines in Fig. 3) and considering the eigenstates of the transfer matrices associated to each segment. These eigenstates, whose transverse field distributions are invariant under the propagation over one segment, also represent the Bloch modes associated to the periodic structure formed by a series of identical segments [17]. Within this picture, designing a taper amounts to implementing a progressive variation of the transverse Bloch mode profile through a series of segments, from the profile of the fundamental guided mode of the air-bridge to that of the

#5572 - $15.00 US Received 25 October 2004; revised 22 December 2004; accepted 30 December 2004

evanescent Bloch mode associated to the periodic mirror. A more detailed analysis on the tapering by engineering evanescent Bloch modes can be found in Ref. [17], where the key role played by the fundamental Bloch mode of every segment in the loss reduction has been quantitatively addressed for simpler 2D geometries.

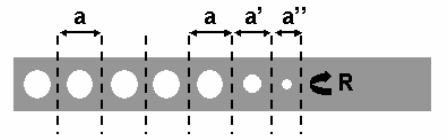

Fig. 3. Illustration of geometry tuning for tapering. Two segments of length a' and a'' are inserted between the PC mirror and the air-bridge.

Apart from refractive index modulations, which may be difficult to implement in practice, two degrees of freedom can be varied for the taper design, namely the segment length and the hole diameter. Figure 4(a) shows the overlap integral (1-η is shown in a logarithmic scale) between the air-bridge guided mode and the half-Bloch waves associated to three segments with different hole diameters, d = 230, 170 and 100 nm. The computation is performed for a given wavelength, λ = 1.5 μm, and the displayed data correspond only to evanescent Bloch modes, i.e. Bloch modes operating in the gap. A priori, segments involving non-evanescent Bloch modes could be considered for the design. However, restricting a design to segments supporting only evanescent Bloch modes amounts to considering mirrors with short penetration length, a desirable feature for cavities with ultra small modal volume or very large finesse. The general trends in Fig. 4(a) are rather intuitive: 1) for a given hole diameter, the overlap integral η increases as the segment length a decreases, see also Fig. 2 and 2) η increases as the diameter decreases, an expected trend if one considers that the segment and the air-bridge becomes identical in the zero hole-diameter limit. If one associates to every η in Fig. 4(a) a transverse mode profile, one easily realizes that a continuum of mode profiles can be envisioned for the tapering process, ranging from the Bloch mode profile of the Bragg mirror (vertical arrow in Fig. 4(a)) to the air-bridge mode profile which is likely to be very similar to that of the segment with the smallest length and hole diameter.

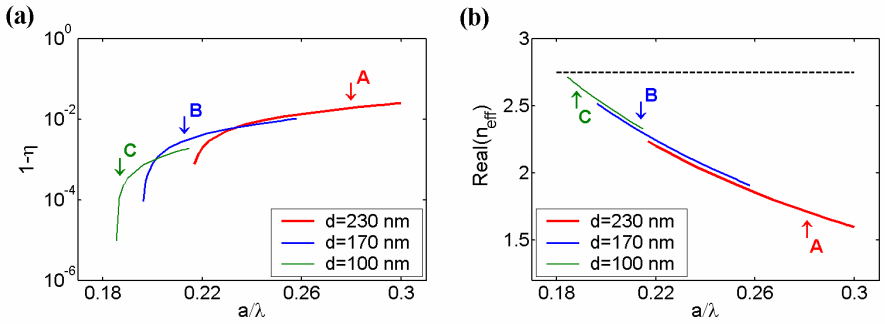

Fig. 4. Relevant quantities for the evanescent Bloch mode associated to three segments with different hole diameters, d = 230, 170 and 100 nm, for λ = 1.5 μm. (a) 1-η as a function of the segment period. (b) Real part of the effective index n_{eff} of the Bloch mode of the segments. The curves for d = 230 and 170 nm are down shifted by 0.07 and 0.03, respectively, for the sake of clarity [otherwise, Real(n_{eff}) = $\lambda/(2a)$]. The horizontal dashed line represents the effective index of the fundamental air-bridge guided mode. The vertical arrow labelled A indicates the location associated to the mirror with a 420-nm period. The vertical arrows labelled B and C indicate the location associated to the segments used in Section 4.2 to reduce the losses.

Until now, we have considered the transverse mode profile of the half-Bloch wave since, strictly speaking, it is the primary quantity to be dealt with for the taper design. A simpler and more intuitive quantity, which may be more useful in practice although less quantitative, is the

#5572 - $15.00 US Received 25 October 2004; revised 22 December 2004; accepted 30 December 2004

real part of the effective indices n_{eff} of the Bloch modes involved in the taper. These effective indices are shown in Fig. 4(b). Their values, which are given by $n_{eff} = \lambda/(2a)$ for Bloch modes in the gap [17, 30], increase as the segment lengths decrease. If we admit that a progressive effective index variation is accompanied by a progressive variation of the transverse Bloch mode profiles, the design of the taper amounts to implementing a graded-index Bloch-mode stack from the effective index of the guided mode to that of the Bloch mode of the mirror. In the next Section, we will show that taper designs can be basically hand-driven using the effective index approach.

4. Numerical evidence

In this Section, we provide numerical evidence of modal reflectivity enhancement through evanescent Bloch-mode engineering. For implementing a mirror taper, tuning both segment-length *a* and hole-diameter *d* have to be considered. Section 4.1 is concerned by tapers based on a simple hole shift at the mirror termination. Geometries such as 1D Bragg reflectors in rectangular photonic wires and 2D PC mirrors in membranes are considered. In Section 4.2, more sophisticated tapers involving a tuning of both *a* and *d* are considered for photonic wires.

4.1. Tuning hole position

The primary degree of freedom for modifying the transverse mode profile of evanescent Bloch modes operating in the gap is the periodicity constant. This assertion is derived from Fig. 4(a), where the overlap integral is shown to vary by several order of magnitude by tuning the periodicity constant for a fixed hole diameter. In practice, when inserting a single segment between a periodic mirror and a waveguide, tuning the periodicity constant of the segment amounts to shifting the hole position, and implementing a graded variation of the transverse mode profile is achieved with a segment whose length is shorter than the periodicity of the mirror, see Fig. 4. Hereafter, this simple design rule is studied for 1D Bragg reflectors in rectangular photonic wires and 2D PC mirrors in membranes.

Let us first consider the reflection problem shown in Fig. 5(a), where a 2D PC mirror is illuminated by the fundamental Bloch mode of a single-line defect PC waveguide. We assume that the PC mirror is composed of a triangular lattice of air holes (lattice constant a = 420 nm) etched into a silicon slab, whose refractive index n = 3.42 is assumed to be independent of the wavelength in the narrow spectral range of interest. The slab thickness and the air hole radius are 0.6a and 0.29a, respectively. For this set of parameters, the PC waveguide supports a single guided Bloch mode. This mode has been widely studied [28, 31-32]: for $\lambda > 1.5$ µm, it is a truly lossless guided mode operating below the light line of the air-clad. This guided mode is highly dispersive: its group velocity is c/4.5, c/5.4 and c/30 for λ = 1.5, 1.54 and 1.585 µm, respectively, and is null for λ = 1.591 µm at the edge of the first Brillouin zone. As long as the group velocity of the incident guided mode is close to c/3 (a situation referred to as refractive-index guided mode in Ref. [32]), the geometry of Fig. 5a is conceptually similar to that of the air-bridge geometry shown in Fig. 5(b). For instance, the Bloch mode profile of the PC waveguide is very close to the guided mode profile of the air-bridge. We therefore expect that the taper design rules presented in Section 3 remains valid for this 2D PC slab structure.

Figures 5(c)-5(f) summarize the impact of hole displacement on the mirror performance. As shown in Fig. 5(c), the modal reflectivity R_1 slowly increases for small hole shifts, passes through a maximum for $s \approx 0.18a$ and then rapidly drops. Figure 5(e) shows the modal reflectivity spectrum $R_1(\lambda)$ for two hole shifts, $s = 0$ (periodic mirror) and $s = 0.18a$. It is interesting to compare these trends with those obtained for an air-bridge mirror with similar geometrical parameters, see Fig. 5(b). For the comparison, the parameters of the air-bridge mirror are chosen identical to those of the 2D PC slab, a hole periodicity of a, a bridge thickness of 0.6a and a hole radius of 0.29a. The air-bridge width, $w = 1.6a$, is chosen so that the fundamental effective index of the PC waveguide and that of the air-bridge waveguide are equal for λ = 1.5 µm. The effect of hole shifts on the air-bridge-mirror reflectivity R_2 is shown

#5572 - $15.00 US Received 25 October 2004; revised 22 December 2004; accepted 30 December 2004

in Figs. 5(d) and 5(f). The modal reflectivities R_1 and R_2 share many common trends: for $s = 0$, R_1 and R_2 both increase as the wavelength increases and they are both enhanced by small hole shifts before rapidly dropping for large s. This rapid drop is understood if one considers that for large hole shifts, the mode-profile engineering tool does not apply anymore since the fundamental Bloch mode of the additional segment of length a-2s is no longer evanescent. Although R_1 and R_2 share many features, they also exhibit some differences. As shown by a comparative glance at Figs. 5(e) and 5(f), R_1 is larger than R_2 (except for small wavelengths). One is naturally inclined to attribute this trend to the fact that some lateral radiation in the clad which is allowed in the air-bridge geometry is blocked by the 2D PC configuration. This interpretation might be true. However one has to additionally consider that, whereas the group velocity of the fundamental guided mode of the air-bridge waveguide is roughly constant over the whole spectral range of interest, that of the fundamental Bloch mode of the single-line defect PC waveguide drastically changes. In our opinion, this group velocity difference also impacts the modal reflectivity spectrum. Theoretically, it can be shown that, as $v_g \rightarrow 0$, the modal reflectivity of any guided (non-leaky) Bloch mode which approaches the edge of the first Brillouin zone is unity (the modal reflectivity coefficient is -1). The main physical reason is a degeneracy: the Bloch mode and its associated counter-propagating wave are identical. We have confirmed this through many computational results obtained for 2D grating waveguide geometries. For the 3D geometry of Fig. 5(a), the calculation is much more technically difficult and we were unable to calculate the modal reflectivity R_1 for $\lambda > 1.585$ µm ($v_g = c/30$). But R_1 is expected to reach unity for $\lambda = 1.591$ µm ($v_g = 0$) and for any value of s.

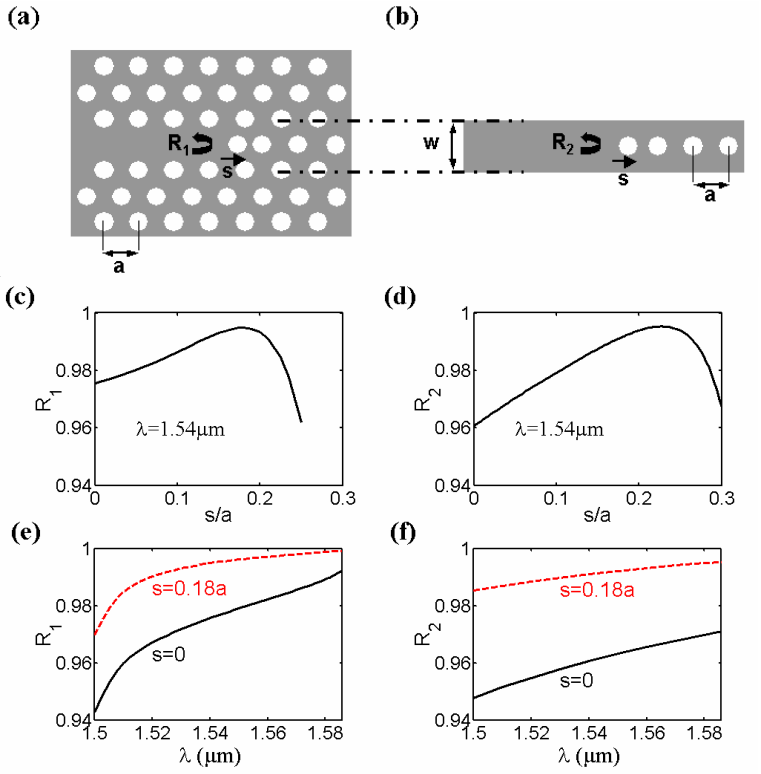

Fig. 5. Effect of hole shifting on the modal reflectivity of 1D and 2D PC mirrors. (a) 2D PC configuration. (b) Related air-bridge configuration. (c) and (d) Modal reflectivities R_1 and R_2 for $\lambda = 1.54$ µm as a function of the normalized hole shift s/a. (e) and (f) Corresponding modal reflectivity spectra. The solid and dashed curves are obtained for $s = 0$ and $s = 0.18$a, respectively.

#5572 - $15.00 US Received 25 October 2004; revised 22 December 2004; accepted 30 December 2004

Finally, let us note that the very high reflectivity observed for the 2D PC mirror ($R_1 \approx 0.998$) for $\lambda \approx 1.58$ µm and for $s = 0.18a$ is responsible for the very high Q factor in excess of 45,000 observed experimentally [14] with a cavity formed by removing three holes in a 2D PC etched into a silicon membrane, as discussed in Ref. [33]. We also believe that the recent observation [8, 34] of quality factor enhancement in single-hole defect cavities in a 2D PC membrane by hole tuning around the defect is likely to be related to the mode-profile matching approach described here.

4.2. Tuning hole position and diameter

In this subsection, we consider more sophisticated tapers involving one or two segments with a tuning of both the segment length and the hole diameter. We first consider 1D Bragg reflectors in the micropillar geometry of Fig. 1(b). While the mode lifetime of micropillars with small refractive-index modulations (like those manufactured with quarter-wave stacks in the GaAs/AlAs system) weakly suffers from mode-profile mismatch problems [35], the problem is radically different for high refractive index modulations. For example, for the GaAs/AlO_x system, the transverse mode profile of the HE_{11} (i.e., fundamental) guided mode of the cylindrical photonic wire (the cavity spacer in Fig. 1(b)) strongly differs from that of the associated Bloch mode in the Bragg reflector. Thus a strong mode-profile mismatch exists and large cavity quality factors are prohibited. Although not argued in these terms, numerical results have confirmed this prediction [36]. This mode-profile mismatch can be reduced with a single segment taper. To confirm this, we consider a 1D Bragg reflector formed in a 800-nm-diameter pillar composed of GaAs and AlO_x layers, with refractive indices 3.495 and 1.515 and thicknesses $d_1 = 78$ nm and $d_2 = 150$ nm, respectively. For this set of parameters, see Fig. 6(a), a 420 nm wide bandgap is obtained around a centre wavelength $\lambda = 0.95$ µm. For a semi-infinite Bragg reflector, we have calculated the modal reflectivity R_3 of the HE_{11} guided mode of the cylindrical photonic wire for the midgap frequency and for several values of the first GaAs and AlOx layers thicknesses, noted x_1 and x_2, respectively. The modal reflectivity of the periodic mirror ($x_1 = d_1$ and $x_2 = d_2$) is 95.7%, see the point A in Fig. 6b; a maximum reflectivity of 98.3% is achieved for $x_1 = 95$ nm and $x_2 = 50$ nm (point B). Thus by varying both x_1 and x_2, the radiation loss $L = 1\text{-}R_3$ are reduced by roughly a factor 3. This implies that the quality factor of a cavity formed by the association of two mirrors would be increased by the same amount.

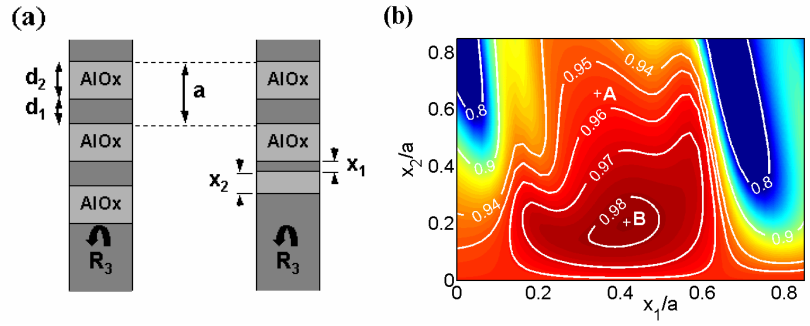

Fig. 6. Single-segment tapers for micropillar Bragg reflectors. (a) Reflector geometry ($a = d_1 + d_2 = 228$ nm). Dark and light regions correspond to GaAs and AlO_x materials. (b) Modal reflectivity as a function of the normalized thicknesses x_1/a and x_2/a of the first GaAs and AlOx layers for $\lambda = 0.95$ µm. Points A and B correspond to geometries with periodic and optimized mirrors, respectively.

We now consider two-segment tapers formed in the air-bridge geometry of Fig. 3 and report on a drastic reduction of the radiations losses in comparison to single-segment tapers formed in the same geometry. For a nominal wavelength of 1.5 µm, two designs are reported.

#5572 - $15.00 US Received 25 October 2004; revised 22 December 2004; accepted 30 December 2004

The first one is hand-driven and exploits the data of Fig. 4. We have selected two segments with a = 320 nm and d = 170 nm, and a = 280 nm and d = 100 nm. These segment geometries are shown by the vertical arrows labelled B and C in Figs. 4a and 4b. The choice is largely arbitrary, but the choice of the first segment is motivated by the realisation of a taper with very low losses, see Fig. 4(a), and the choice of the second segment is mainly motivated by the realisation of a graded-index operation. With the Fourier modal method, we have calculated the modal reflectivity spectrum of the mirror, bold curve in Fig. 7. For the second design, we have used Simulated-Annealing [37] procedure and have optimised the modal reflectivity. In the optimisation, four degrees of freedom are used: the two hole diameters and the two hole positions, under the constraint that the hole diameters remain larger than 100 nm. Because of the large amount of computational loads required for the optimisation, we have not explored thoroughly the configuration space. Several taper geometries with very high reflectivities at the design wavelength have been obtained. The mirror reflectivity spectrum of one of these optimised tapers is shown as the thin curve in Fig. 7.

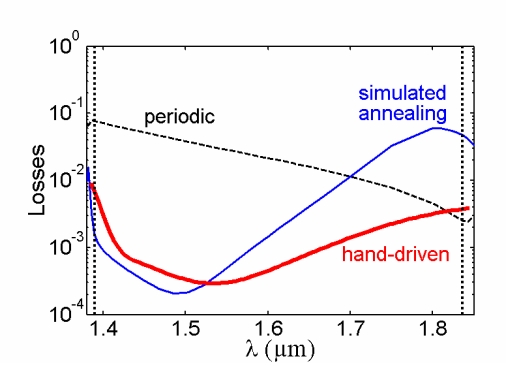

Fig. 7. Radiation loss spectra L = 1-R for air-bridge mirrors with two-segment tapers. Red bold curve: hand-driven design for segments defined by (a', d) = (320, 170) nm, and (a'', d) = (280, 100) nm. Blue thin curve: optimized design for segments defined by (a', d) = (240, 210) nm, and (a'', d) = (414, 100) nm. The dashed curve corresponds to the modal reflectivity of the periodic mirror and the vertical dotted lines indicate the band edge.

These numerical results clearly evidence the beneficial effect of two-segment tapering processes: a loss reduction by a factor larger than 200 at the design wavelength and by one order of magnitude ($L < 10^{-3}$) over a broad spectral range. We believe that many different taper geometries may lead to a drastic reduction of the radiation losses and therefore that tapers designed by use of a graded mode-profile variation are not very sensitive to fabrication errors of the hole diameters, as shown in Ref. [17] for related 2D geometries.

5. Conclusion

The modal reflectivities of several PC mirrors, including 1D Bragg reflectors in cylindrical and rectangular photonic wires and 2D PC mirrors in membranes, have been theoretically studied. The deviation of the modal reflectivity from unity, which represents radiation losses in the cladding materials, has been shown to result from a transverse mode-profile mismatch at the waveguide-mirror interface. Indeed, losses derived from overlap integral considerations show excellent agreement with those predicted by a full 3D calculation. Design tools based on an engineering of the Bloch modes in the mirrors through geometry tuning have been proposed for reducing these losses. Efficient tapered mirrors providing a loss reduction by one or two orders of magnitude have been validated through 3D computational results. The design tools can be applied to enhance the quality factor of various optical microcavities like air-bridge microcavities, micropillars and 2D PC microcavities in membranes. In addition, because the tapering process relies on evanescent Bloch modes operating in the gap, the penetration length into the engineered mirrors is kept at a rather low level. Thus the modal

#5572 - $15.00 US Received 25 October 2004; revised 22 December 2004; accepted 30 December 2004

volumes of cavities formed by two engineered mirrors are not substantially increased in comparison to those of cavities formed by fully periodic mirrors.

Acknowledgments

C. Sauvan is grateful to the Délégation Générale pour l'Armement for his PhD fellowship. The authors acknowledge financial support from Action Concertée Nanoscience 2004, French Ministry in charge of Research. The authors thank Pierre Chavel for his helpful critical review of the manuscript.

#5572 - $15.00 US Received 25 October 2004; revised 22 December 2004; accepted 30 December 2004